

Electronic and magnetic properties of the monoclinic phase BiCrO_3 from first-principles studies

This article has been downloaded from IOPscience. Please scroll down to see the full text article.

2009 J. Phys.: Condens. Matter 21 236006

(<http://iopscience.iop.org/0953-8984/21/23/236006>)

View [the table of contents for this issue](#), or go to the [journal homepage](#) for more

Download details:

IP Address: 129.252.86.83

The article was downloaded on 29/05/2010 at 20:09

Please note that [terms and conditions apply](#).

Electronic and magnetic properties of the monoclinic phase BiCrO_3 from first-principles studies

Yuanhui Xu^{1,2}, Xianfeng Hao¹, Jian Meng³, Defeng Zhou^{2,4} and Faming Gao^{1,4}

¹ Department of Chemical Engineering, Yanshan University, Qinhuangdao 066004, People's Republic of China

² School of Biological Engineering, Changchun University of Technology, Changchun 130012, People's Republic of China

³ Key Laboratory of Rare Earth Chemistry and Physics, Changchun Institute of Applied Chemistry, Chinese Academy of Sciences, Changchun 130022, People's Republic of China

E-mail: defengzhou65@126.com and fmgao@ysu.edu

Received 10 March 2009, in final form 24 April 2009

Published 13 May 2009

Online at stacks.iop.org/JPhysCM/21/236006

Abstract

Based on density functional theory, we systematically studied the electronic and magnetic properties of the real experimental structural phase BiCrO_3 with the space group $C2/c$. It is found that the ground state is a moderately correlated Mott–Hubbard insulator with G-type antiferromagnetic structure, which is in agreement with the experimental observations. The magnetism can be qualitatively understood in terms of the superexchange mechanism via $\text{Cr1}(t_{2g})\text{--O } 2p\text{--Cr2}(t_{2g})$. Moreover, the total energies calculated for various magnetic orderings lead to an estimate of the magnetic interaction constants.

(Some figures in this article are in colour only in the electronic version)

Multiferroic materials have simultaneous (anti)ferromagnetic, (anti)ferroelectric, and/or ferroelastic characteristics in the same phase [1]. Coupling between the magnetic and ferroelectric order parameters can lead to magnetoelectric effects, which can be conveniently utilized to tune the electric properties of the materials via applied magnetic field, or vice versa. The recent interest in magnetoelectric materials has been stimulated by their great potential for future multifunctional device applications and fascinating physics. Especially interesting are Bi-containing perovskite-type transition-metal oxides, which have been regarded as the most promising multiferroic materials. In these systems, the ferroelectricity is known to originate from a relative Bi–O displacement resulting from the stereochemical activity of the lone pair on the Bi cations. Some of this series, such as BiFeO_3 [2, 3], BiCoO_3 [4, 5], BiNiO_3 [6, 7], and BiMnO_3 [8, 9], have been extensively studied both experimentally and theoretically.

Despite enormous research efforts, not all the mysteries of these materials, especially, for example, BiCrO_3 , are

known today, and the magnetism and ferroelectricity of BiCrO_3 are still debated [10–14]. The origin of the controversy may be associated with the lack of definite crystal structural information, which is an important prerequisite for understanding the magnetism and ferroelectricity of BiCrO_3 . Very recently, Belik *et al* reinvestigated the crystal and magnetic structures of BiCrO_3 by using the Rietveld method from neutron diffraction data measurements [15]. The results unambiguously indicated that BiCrO_3 crystallizes in the orthorhombic phase above 420 K, and below 420 K down to 7 K, it shows a monoclinic structure with the space group $C2/c$, shown in figure 1 (left). We note that space group $C2/c$ is centrosymmetric and does not support ferroelectricity. In addition, the neutron diffraction data also proved that BiCrO_3 possesses antiferromagnetic long-range order with the magnetic transition temperature $T_N = 109$ K. The magnetic structure is of the Wollan–Koehler [16] G-type with the magnetic moments directed along the monoclinic b axis. Theoretically, although Hill *et al* predicted that BiCrO_3 should have the G-type antiferromagnetic ground

⁴ Authors to whom any correspondence should be addressed.

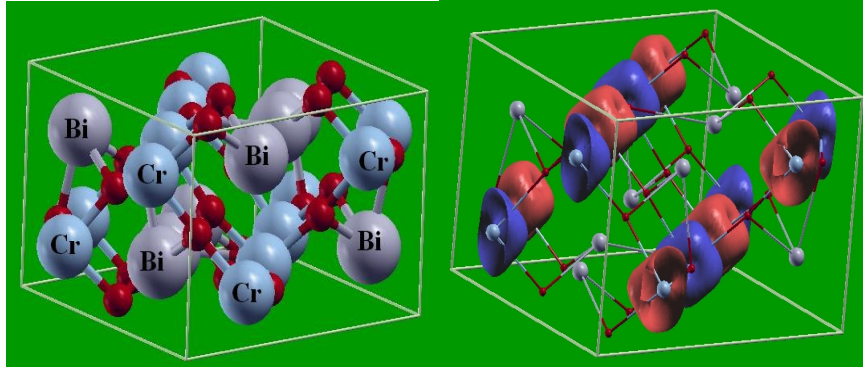


Figure 1. Crystal structure of BiCrO_3 (left), where the Bi, Cr, and O ions are denoted by spheres of decreasing size. On the right is the spin density plot of the G-AFM state, in which the different colors of the Cr atoms indicate spin-up or -down.

state and the antiferrodistortive or antiferroelectric structural distortion [17], their results were obtained on the basis of the hypothetically cubic crystal structure. Therefore, further theoretical investigations on the electronic and magnetic properties for this system based on the new structures determined by Belik *et al* are highly desirable. In this work, we used first-principles density functional calculations to study the electronic and magnetic properties of the monoclinic phase BiCrO_3 . Our results clearly reveal that the ground state of this compound is a Mott–Hubbard insulator with the G-type antiferromagnetic (G-AFM) structure. Furthermore, the mechanism of the magnetic interaction in BiCrO_3 is established.

The calculations were performed within the framework of density functional theory (DFT) utilizing the full-potential linearized augmented plane wave plus local orbital (FP-LAPW + lo) method [18, 19], implemented in the WIEN2k package [20, 21]. We adopted the standard generalized gradient approximation (GGA) within the Perdew–Burke–Ernzerhof 96 scheme [22]. For modeling of the on-site Coulomb correlation for Cr 3d electrons, the GGA + U method [23–25] is used, which combines the GGA approach with the Hubbard model that is especially suitable for treating strongly correlated transition-metal systems. The values of the atomic sphere radii (R_{MT}) were chosen as 2.45, 1.97, and 1.75 au for Bi, Cr, and O atoms, respectively. In order to achieve energy convergence, the wavefunctions in the interstitial region were expanded in plane waves with a cutoff $R_{\text{MT}}^{\text{min}} K_{\text{max}} = 7$, where $R_{\text{MT}}^{\text{min}}$ denotes the smallest atomic sphere radius and K_{max} gives the magnitude of the largest K vector in the plane wave expansion. The valence wavefunctions inside the spheres were expanded up to $l_{\text{max}} = 10$ while the charge density was Fourier expanded up to $G_{\text{max}} = 14$. The number of k points in the whole Brillouin zone was set to 200, resulting in 44 k points in the irreducible Brillouin zone. Self-consistency was considered to be achieved only when the total energy difference between succeeding iterations is less than 10^{-5} Ryd/f.u., while the convergence with respect to charge is less than 10^{-4} . All our results are well converged with respect to k -point mesh and the energy cutoff for the plane wave expansion. The present set-up has been checked to ensure a sufficient accuracy of the

calculations. The lattice parameters and atomic positions used in the calculations were taken from the literature [15].

The GGA + Hubbard U approach has been successful in treating static correlations in transition-metal oxides, however, the selection of an appropriate U_{eff} is rarely straightforward, and a number of methods exist for determining suitable values. These include experimental measurements from photoemission spectroscopy, self-consistent calculations and educated guesswork. In this work, except where otherwise noted, the electronic and magnetic structure were fixed to those obtained by using $U_{\text{eff}} = 3.0$ eV for the treatment of the Cr d orbitals. It should be pointed out that the U_{eff} value we used was adapted from a work about the electronic and magnetic properties of BiCrO_3 based on the hypothetically rhombohedral R3c symmetry [10]. Moreover, the results show that the calculated spin magnetic moment per Cr ion is $2.56 \mu_{\text{B}}$, which is in agreement with the experimentally refined value of $2.55 \mu_{\text{B}}$. Therefore, we concluded that the value of $U_{\text{eff}} = 3.0$ eV for this system is reasonable.

In order to clarify the magnetic ground state in BiCrO_3 , the following magnetic configurations are considered, i.e. the artificial nonmagnetic (NM) configuration by enforcing spin degeneracy for all species; ferromagnetic (FM) ordering and two antiferromagnetic (AFM) orderings, including the G-type AFM phase in which the neighboring magnetic moments couple antiferromagnetically, and the A-type AFM phase with antiferromagnetic interplanar and ferromagnetic intraplanar coupling. A summary of the total energy calculations is given in table 1, where we report the differences in the total energy among the four cases listed earlier. We take the energy of the G-type AFM as our zero energy. The results indicate that the magnetic ground state of BiCrO_3 is the G-type AFM configuration, irrespective of the calculation methods (within the GGA or GGA + U approximation).

To get an insight into the electronic properties of BiCrO_3 within the $C2/c$ space group, we first investigate the experimentally inaccessible NM and FM phases, which can provide a useful reference for understanding the spin-polarized electronic structure. In figure 2(a), the large electronic density of states (DOS) at the Fermi level in the NM configuration suggests that this phase is metallic and should be unstable toward spin polarization based on Stoner’s

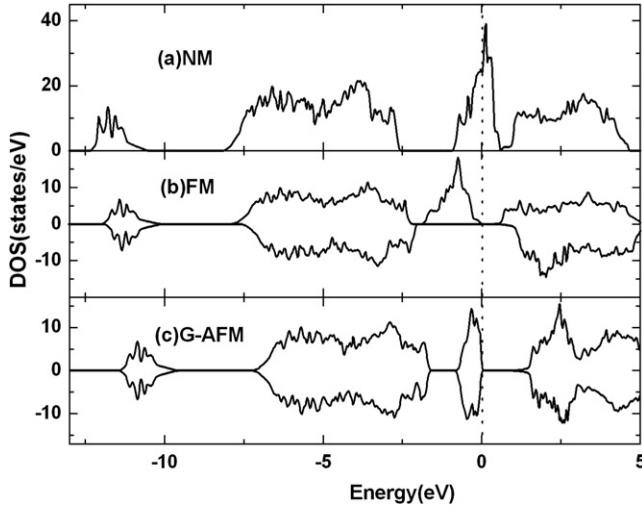


Figure 2. Total density of states (DOS) for the NM, FM, and G-AFM phases calculated by GGA. The Fermi level is set to be zero.

Table 1. Total energies for BiCrO₃ with the different magnetic orderings relative to the G-type antiferromagnetic (G-AFM) configuration in meV/f.u. and the corresponding magnetic exchange interaction constant (meV). Based on the knowledge of J_1 and J_2 , the Néel temperature T_N (K) for the G-type AFM is evaluated from molecular field theory.

Magnetic configurations	GGA	GGA + U ($U_{\text{eff}} = 1$ eV)	GGA + U ($U_{\text{eff}} = 3$ eV)
NM	672		
FM	49.7	42.1	32.2
G-AFM	0	0	0
A-AFM	41.6	35.7	27.6
J_1	1.839	1.558	1.191
J_2	-0.23	-0.21	-0.17
T_N	402	345	267

theory [26]. Figure 2(b) presents a semiconducting FM state with a gap of ~ 0.5 eV, which reveals that spin polarization leads to the opening of a gap in band structure even at the GGA level without considering the on-site Coulomb repulsion U . Indeed, the total energy of the FM phase is lower than that of the NM one (see table 1). However, the ground state of BiCrO₃ is found to be the G-AFM structure, which is more favorable in energy than the FM configuration. Compared to the FM one, figure 2(c) displays a larger band gap (about 1.4 eV) for the G-AFM phase. Note that the Cr 3d DOS curve is sharper and has an obvious shift to the Fermi level, indicating a localized character of Cr 3d electrons. It is generally believed that the conventional GGA method is inadequate to describe the electronic structure of materials with partially filled d or f valence states. Since this method cannot take the self-interaction correction into account, it always fails to reproduce the insulating behavior, or underestimates the band gap and the magnetic moments for many perovskites. Therefore, it is necessary to take the GGA + U approximation further to treat this system.

Figure 3 presents the total and site-decomposed DOS of the G-type AFM configuration within the GGA + U approach.

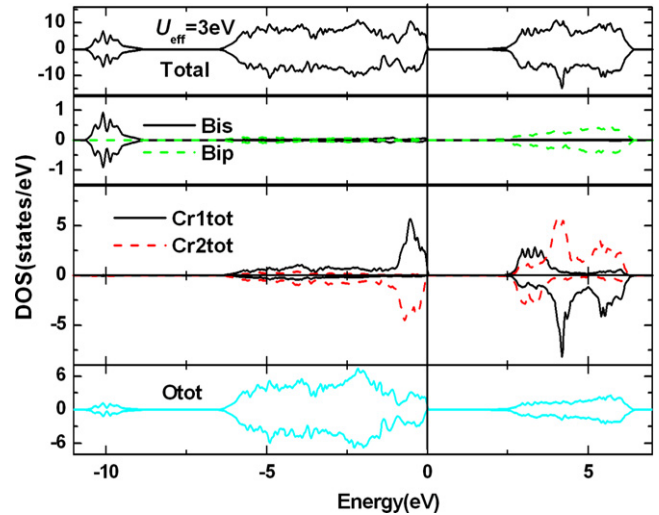


Figure 3. Site-decomposed DOS of BiCrO₃ in the G-AFM state obtained from the GGA + U ($U_{\text{eff}} = 3$ eV) method. Zero energy is set as the Fermi level.

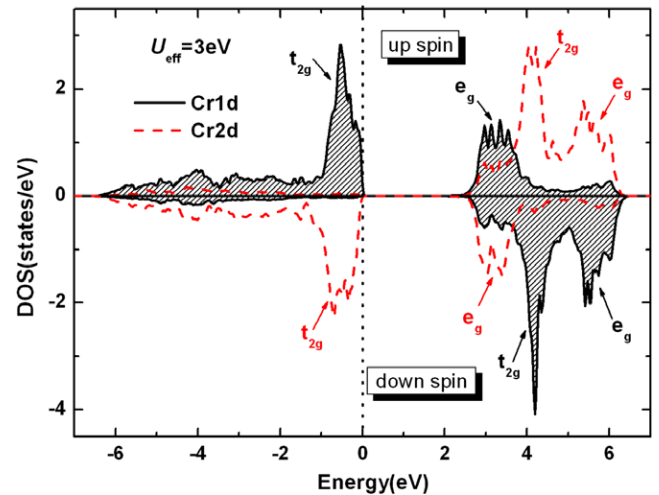


Figure 4. Orbital-resolved DOS of Cr 3d levels in the G-AFM structure obtained using GGA + U ($U_{\text{eff}} = 3$ eV).

In the presence of the on-site Coulomb interaction, as expected, the occupied bands lowered in energy and the unoccupied bands raised, thereby increasing the band gap. Obviously, a split-off peak at approximately -10 eV corresponds to Bi 6s lone-paired electronic states, while Bi 6p states lie in the high energy region well above the Fermi level, reflecting an ionic nature for the Bi atom in this system. Additionally, the energy region between -6 and -1 eV is mainly formed by O 2p states with a bonding hybridization with Cr 3d states. Cr 3d states give predominant contributions to the bands around the Fermi level. One can see that the band gap above the Fermi level is located between the Cr d orbitals. Thus, we may conclude that the ground state of BiCrO₃ should be a Mott–Hubbard insulator.

It is of interest to look at the orbital behavior of the transition-metal Cr atom in the G-AFM structure. Figure 4 shows the orbital-resolved DOS for the Cr 3d level. Note

that the Cr1 and Cr2 atoms with opposite spin directions have different topologies of DOS, which is due to their different crystallographical sites. The fivefold Cr 3d level is split by the crystal field into t_{2g} and e_g subbands, as labeled in the plot. Obviously, the t_{2g} band is fully occupied and e_g completely unoccupied in one spin direction while they are all empty in the other spin direction, which accounts for the nominally 3+ valency for Cr atoms in BiCrO_3 . In addition, the exchange splitting energy between the spin-up and-down Cr 3d bands is found to be roughly 4.5 eV, which is larger than that of the crystal field splitting value of about 3.0 eV. Moreover, the calculated spin magnetic moment per Cr ion is only $2.56 \mu_B$ inside the atomic sphere, which is less than the expected value of $3 \mu_B$ for a $\text{Cr}^{3+}(3d^3)$ ion mainly due to the strong hybridizations with the O atoms.

In order to explore the magnetic interaction in the ground state of BiCrO_3 , we evaluate the magnetic interaction constants by computing the difference of total energy per Cr atom between the FM, G-type AFM, and A-type AFM orderings within the classic Heisenberg spin Hamiltonian

$$H_{\text{ex}} = \sum_{i,j} J_{ij} S_i S_j$$

where the sum is extended over i, j (i.e. each pair appears twice). $J < 0$ and $J > 0$ for, respectively, FM and AFM exchange interaction and $S = 3/2$ is the spin of the Cr^{3+} atom characterized by a $3d^3$ electronic configuration. The values of the exchange parameters are obtained by computing the difference of total energy among various magnetic orderings. The number of orderings is determined by the number of exchange constants in the above equation. Here, we limit ourselves to nearest-neighbor (nn) J_1 and next-nearest-neighbors (nnn) J_2 interactions for the three different magnetic configurations, as listed in table 1. In the three-dimensional long-range ordered magnetic structure of BiCrO_3 , then, each Cr atom has six nn and twelve nnn spin exchange interactions. For simplicity, we assume that all six nn interactions are identical, and so are all the twelve nnn interactions. Within the GGA + U ($U_{\text{eff}} = 3.0$ eV) approach, it turns out $J_1 = 1.191$ meV and $J_2 = -0.17$ meV, which means the nearest-neighbor interaction is antiferromagnetic and the next-nearest-neighbor interaction is very weak ferromagnetic. This is in accordance with the coupling between the Cr ions in the G-AFM structure, which can also be seen from the spin density plot presented in figure 1 (right). The variation in the spin exchange constants as a function of Hubbard U is also listed in table 1. Since the AFM exchange interaction is proportional to $1/U$, as U increases, all the exchange interaction constants decrease. Moreover, the accuracy of these estimates is tested by calculating the magnetic transition temperature T_N within the molecular field theory [27, 28]:

$$T_N^{\text{G-AFM}} = \frac{2S(S+1)}{3k_B} |-6J_1 + 12J_2|$$

where k_B is the Boltzmann constant. In the presence of on-site Coulomb interaction ($U_{\text{eff}} = 3.0$ eV), the Néel temperature of the G-AFM phase, $T_N = 267$ K, is twice as large as the experimental measurement of $T_N = 109$ K, at which the

incipient AFM interaction appears experimentally. It should be mentioned that the molecular field theory yields an upper bound for the Néel temperature, as the electronic fluctuations are neglected. The experimentally measured temperature is thus expected to be lower than the predicted one.

The Goodenough–Kanamori–Anderson (GKA) rules [29, 30] pointed out that the exchange interaction between the half-filled orbitals of the transition-metal ions through the surrounding oxygen ligands typically can lead to superexchange interactions in magnetic perovskites, which should be relatively strong and antiferromagnetic. In our case, note that the spin exchange interaction between the Cr atoms is through the O 2p orbitals and the angles of the Cr1–O–Cr2 bonds lie in the range from 152° to 160° [15]. Also the Cr atom possesses the half-filled t_{2g} orbital with $3d^3$ electronic configuration in BiCrO_3 , so one can reach the conclusion that the nn spin interaction between the Cr atoms is antiferromagnetic, which is attested by the magnetic interaction constants' calculation discussed above. Viewed in this light, we can ascribe the magnetic interactions of BiCrO_3 to the superexchange mechanism via Cr1(t_{2g})–O 2p–Cr2(t_{2g}).

In conclusion, we have investigated the electronic and magnetic properties of BiCrO_3 using first-principles calculations with the GGA and GGA + U approaches. Our results indicate that the ground state of BiCrO_3 is a moderately correlated Mott–Hubbard insulator with the G-type AFM configuration. From the estimation of the magnetic interaction constants, we confirmed that the nearest-neighbor spin interaction is antiferromagnetic while the next-nearest-neighbor interaction is very weakly ferromagnetic, which is consistent with the experimental observation. Additionally, the magnetic exchange interaction in BiCrO_3 can be attributed to the superexchange mechanism.

Acknowledgments

This work received financial support from the National Natural Science Foundation of China (grant Nos 20671088, 20661026, 20871023, and 20831004).

References

- [1] Hill N A 2000 *J. Phys. Chem. B* **104** 6694
- [2] Wang J, Neaton J B, Zheng H, Nagarajan V, Ogale S B, Liu B, Viehland D, Vaithyanathan V, Schlom D G, Waghmare U V, Spaldin N A, Rabe K M, Wuttig M and Ramesh R 2003 *Science* **299** 1719
- [3] Neaton J B, Ederer C, Waghmare U V, Spaldin N A and Rabe K M 2005 *Phys. Rev. B* **71** 014113
- [4] Belik A A, Iikubo S, Kodama K, Igawa N, Shamoto S, Niitaka S, Azuma M, Shimakawa Y, Takano M, Izumi F and Muromachi E 2006 *Chem. Mater.* **18** 798
- [5] Cai M Q, Liu J C, Yang G W, Cao Y L, Tan X, Chen X Y, Wang Y G and Hu W Y 2007 *J. Chem. Phys.* **126** 154708
- [6] Ishiwata S, Azuma M, Takano M, Nishibori E, Takata M, Sakata M and Kato K 2002 *J. Mater. Chem.* **12** 3733
- [7] Cai M Q, Wang G W, Tan X, Cao Y L, Wang L L, Hu W Y and Wang Y G 2007 *Appl. Phys. Lett.* **91** 101901
- [8] Moreira dos Santos A, Parashar S, Raju A R, Zhao Y S, Cheetham A K and Rao C N R 2002 *Solid State Commun.* **49** 122
- [9] Solovoy I V and Pchelkina Z V 2008 *New J. Phys.* **10** 073021

- [10] Baetting P, Ederer C and Spaldin N A 2005 *Phys. Rev. B* **72** 214105
- [11] Belik A A, Ysujii N, Suzuki H and Takayama-Muromachi E 2007 *Inorg. Chem.* **46** 8746
- [12] Murakami M, Fujino S, Lim S-H, Long C J, Salamanca-Riba L G, Wutting M and Takeuchi I 2006 *Appl. Phys. Lett.* **88** 152902
- [13] Kim D H, Lee H N, Varela M and Christen H M 2006 *Appl. Phys. Lett.* **89** 162904
- [14] Niitaka S, Azuma M, Takano M, Nishibori E, Takata M and Sakata M 2004 *Solid State Ion.* **172** 557
- [15] Belik A A, Iikubo S, Kodama K, Igawa N, Shamoto S and Takayama-Muromachi E 2008 *Chem. Mater.* **20** 3765
- [16] Wollan E O and Koehler W C 1955 *Phys. Rev.* **100** 545
- [17] Hill N A, Bättig P and Daul C 2002 *J. Phys. Chem. B* **106** 3383
- [18] Sjöstedt E, Nordström L and Singh D J 2000 *Solid State Commun.* **15** 114
- [19] Madsen G K H, Blaha P, Schwarz K, Sjöstedt E and Nordström L 2001 *Phys. Rev. B* **64** 195134
- [20] Schwarz K and Blaha P 2003 *Comput. Mater. Sci.* **28** 259
- [21] Blaha P, Schwarz K, Madsen G K H, Kvasnicka D and Luitz J 2001 *WIEN2k, An Augmented Plane Wave Plus Local Orbitals Program for Calculating Crystal Properties* (Austria: Vienna University of Technology) ISBN 3-9501031-1-2
- [22] Perdew J, Burke S and Ernzerhof M 1996 *Phys. Rev. Lett.* **77** 3865
- [23] Lichtenstein A, Anisimov V and Zaanen J 1995 *Phys. Rev. B* **52** 5467
- [24] Anisimov V, Aryasetiawan F and Lichtenstein A 1997 *J. Phys.: Condens. Matter* **9** 767
- [25] Petukhov A, Mazin I, Chioncel L and Lichtenstein A 2003 *Phys. Rev. B* **67** 153106
- [26] Matar S F 2003 *Prog. Solid State Chem.* **31** 239
- [27] Smart J S 1959 *Phys. Chem. Solids* **11** 97
- [28] Lampis N, Franchini C, Satta G, Geddo-Lehmann A and Massidda S 2004 *Phys. Rev. B* **69** 064412
- [29] Anderson P W 1963 Exchange in insulators: superexchange, direct exchange, and double exchange *Magnetic Ions in Insulators. Their Interactions, Resonances, and Optical Properties of Magnetism* vol I (New York: Academic)
- [30] Goodenough J B 1963 *Magnetism and the Chemical Bond* (New York: Interscience)